

LUMPED AND DISTRIBUTED
SCALING OF MESFETs

J. P. Mondal

General Electric Company
Electronics Laboratory
Syracuse, NY 13221Abstract

The paper describes a proper way of scaling up large MESFETs starting from elementary cell measurements. The distributed scaling is emphasized and compared with lumped scaling. Experimental results are shown. All the manifold distribution and parasitic effects are accounted for.

Introduction

In power amplifier applications, it is very common to scale up large MESFETs at the output from smaller MESFET devices that are easily measured and characterized. If enough attention is not paid to the scalability of an element, the final device model may differ substantially from the actual device. Care must be taken to account for the manifold distribution effects and other parasitics (like airbridges, distribution of via holes). In this paper, a systematic procedure is given to predict the small signal performance of large devices from the measured and well-characterized elementary cells. The emphasis is on the distributed scaling; the method is compared with lumped scaling. The prediction with distributed scaling showed a good agreement with the measured results. The lumped element approach is very commonly used and able to predict the device performance very well, depending on the device size, feed structure, and the modeled bandwidth.

An assumption is made during the scaling; every gate finger and the associated channel characteristics are identical. For example, in Fig. 1 (elementary two-gate-fingered cell), an RF signal applied at the gate gets split into even modes and then gets combined along the width of the drain finger. No odd mode current flows across the drain finger. The elements in the equivalent circuit model correspond to even mode excitation only.

A selection criterion, based on DC characteristics only, has been set for the devices chosen for experimental verification. We have chosen devices from the same reticle with $\pm 10\%$ normalized DC characteristics. The gate length variation is much less in the same reticle than from reticle to reticle. All other parasitics and distribution effects are dependent on the horizontal layout of the device, which is quite well controlled.

Analysis and Measurement

The basic analytical approach for the distributed modeling has been developed from [1][2] with the proper evaluation of [Z] and [Y] matrices. The drain and gate lines are assumed to be asymmetrically coupled with source as the common ground. So the current flow is along the width of the drain and gate lines and across the width on the source pad. The inductance matrix has been estimated from the capacitance formulae given in [3]. The estimated values are then optimized simultaneously to fit the measured S-parameters of the device over a number of bias points simultaneously [4]. The bonding and via hole parasitics are determined by combining cold and hot FET data simultaneously over seven bias points and comparing between RF-probed data on unthinned substrate and the fixture-mounted data [4]. The measurement should be taken on elementary cells with the least manifold distribution effects. The via hole inductance turns out to be ~ 0.03 nH. Since it is very difficult to maintain the same bondwire inductance from device to device, a very tight tolerance is maintained between two bonding points (8-10 mils), generally with a bond angle of less than 5° . This has a range of inductance between .2 and .3 nH (for .4-mil wire radius). The gate and drain manifolds are considered asymmetric coupled lines with respect to the device fingers and their effects are lumped into L's and C's as shown in Fig. 2 for a four-fingered FET. Lumped element approximation for the manifold and airbridge is possible, because the cutoff frequency associated with such a structure is quite high compared to the measurement frequency range. The distributed model of a single-finger FET is shown in Fig. 3; this model is used inside the dotted box in Fig. 2. Fig. 4(a) shows the fixture deembeded data fit with the lumped and distributed models, along with RF-probed data for a cold FET (400 μm , two fingers). Fig. 4(b) shows the same at a hot bias point. Fig. 4(c) shows the way in which the parasitics have been extracted. The measured frequency range is 2-18 GHz. Table 1 shows the element values. Fig. 5 shows the fit for a 1600 μm device (eight fingers) and Table 2 gives the corresponding values. Note the elements that get modified in the lumped element model, whereas in the distributed case the normalized parameters are almost the same as the previous case. Fig. 6 shows a distributed model fit to a 3200 μm device (16 fingers) at the same bias point as the

previous ones. Its S-parameters could not be fitted with a scaled up lumped element model as in Figs. 4 and 5. For scaling the series elements (R_G , L_G , L_D and R_D) in the lumped element model, we have used the following formula,

$$\frac{X_2}{X_1} = \left(\frac{W_2}{W_1} \right) \cdot \left(\frac{N_1}{N_2} \right)^2$$

where, $W_{1,2}$ = total gate widths
 $N_{1,2}$ = total number of gate fingers
 $X_{1,2}$ = corresponding series elements
 $(R_G, L_G, L_D$ or $R_D)$

In bigger cell optimization, we first hold the $[Z]$ and $[Y]$ matrix/unit length (determined from the elementary cell measurement constant) and optimize for the manifold and airbridge parasitics simultaneously over five bias points; then we let the bias-dependent elements in the $[Y]$ -matrix vary by approximately $\pm 10\%$ to get an overall good fit for all the bias points. This is required to account for device-to-device variation, especially for bigger cells in which there is an averaging out effect, because all the fingers may not be identical.

Conclusion

It is shown with experimental results that with proper methodology, it is possible to predict the larger cell performance by scaling it up from elementary cells. The distributed scaling approach has been applied quite successfully to predict the device performance. In the analysis, we have not taken into account the skin effects on the resistance and the internal inductance of the gate and drain lines. $[R]$ and $[L]$ matrices are assumed constant over the frequency range of interest.

References

- [1] V. K. Tripathi, "Asymmetric Coupled Transmission Lines in an Inhomogeneous Medium," *IEEE Trans. on Microwave Theory and Techniques*, vol. MTT-35, No. 5, May 1987, pp. 487-491.
- [2] J. P. Mondal, "An Experimental Verification of a Simple Distributed Model of MIM Capacitors for MMIC Applications," *IEEE Trans. on Microwave Theory and Techniques*, vol. MTT-35, no. 4, April 1987, pp. 403-407.
- [3] K. C. Gupta et al, "Computer Aided Design of Microwave Circuits," *Artech House*, 1981, p. 281.
- [4] J. P. Mondal and T. H. Chen, "Propagation Constant Determination in Microwave Fixture Deembedding Procedure," *IEEE Trans. on Microwave Theory and Techniques*, vol. MTT-36, no. 4, April 1988.

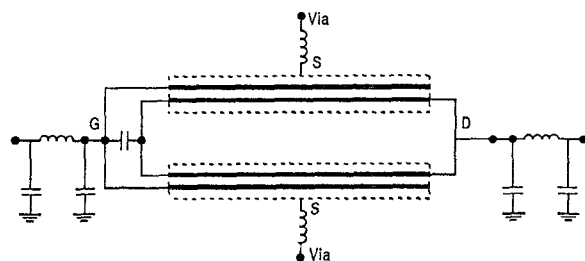


FIG. 1. A two-finger FET with the drain finger split with a magnetic wall. The bonding and via hole parasitics are also shown.

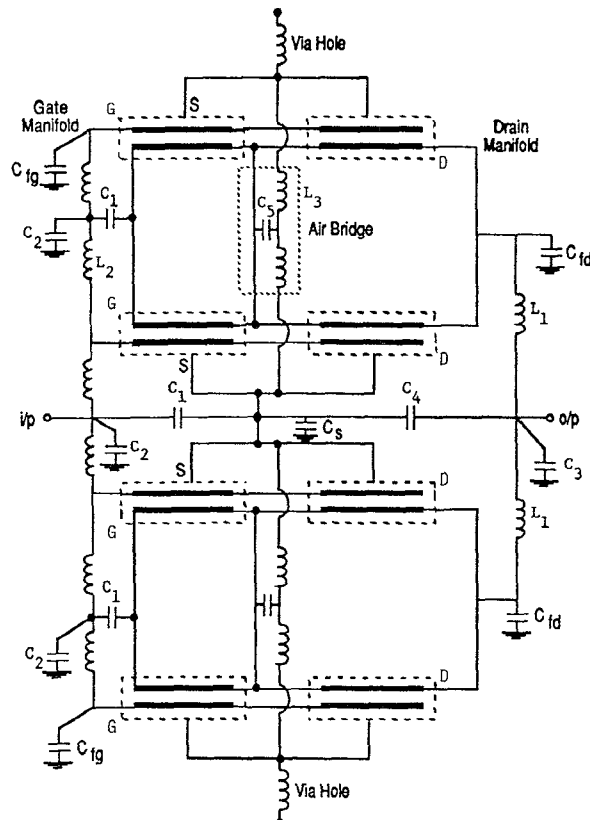


FIG. 2. Semi-distributed modeling of a four-finger FET. Each drain finger is divided strictly with a magnetic wall along the middle of its width (even mode only). C_{fg} and C_{fd} are the fringing field capacitances of the gate and drain manifolds, respectively, which are due to open ended effects of the manifold. On 100 μm GaAs substrate, it is approximately .005 pF/100 μm of periphery.

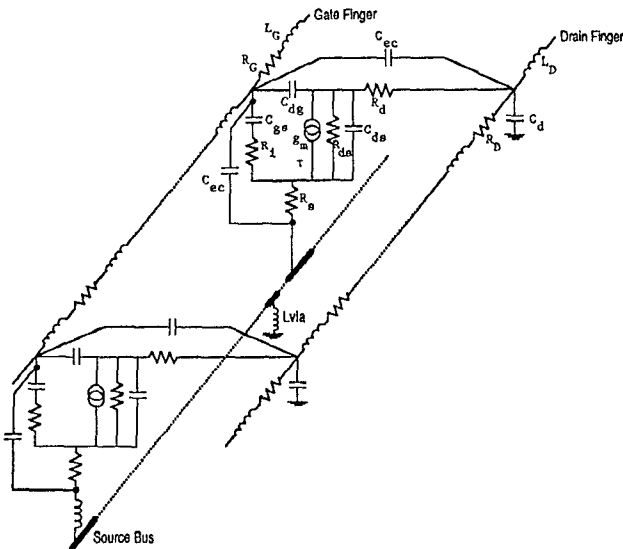


FIG. 3. Distributed modeling of a single-finger FET. The underlying assumption in this sketch is that the current is flowing along the widths of the gate and drain fingers, while on source the current flow is across the width of the finger.

TABLE 1. Lumped and distributed elements for a two-fingered elementary cell (400 μm total gate width).

	BIAS DEPENDENT						BIAS INDEPENDENT									
	C_{dg}	C_{gs}	g_m	R_{ds}	R_i	τ	R_g	L_g	C_{dc}	R_d	R_s	R_p	L_d	C_{ds}	C_d	L_v
LUMPED	.029	.31	.016	492	5.9	5.9	2.48	.08	.0054	1.2	3.1	NA	.09	.078	NA	.014
DISTRIBUTED	.073	.762	.043	190	1.8	6.2	.75	.35	.005	.44	1.44	2.3	.41	.203	.024	.013

BOND PARASITICS						
C_{p+41}	C_{p+42}	C_{g0}	C_{dd}	L_{bg}	L_{bd}	
LUMPED	.028	.035	.044	.045	.26	.29
DISTRIBUTED	.028	.029	.049	.045	.26	.29

All capacitors in pF, all inductors in nH, all resistors in Ω , g_m in mho, τ in ps, distributed elements are all per mm, except bond parasitics, τ , and L_v . Distributed elements are all even mode, except bond parasitics and L_v . Even mode value for L_v is that of a single via hole ($\sim .03$ nH).

* C_{ds} assumes one of two values, depending on the bias condition, either hot or cold.

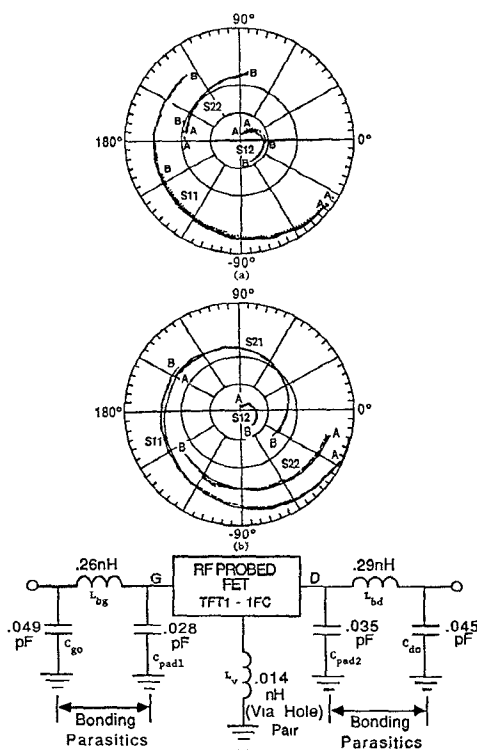


FIG. 4. Sample fitting of lumped and distributed models with fixture desmeared (no wires included). S-parameter data for a 400 μm elementary cell (a) and a 1600 μm cell (b) are shown. Both are fits of seven bias points, optimized simultaneously. For a cold FET, we also show the RF-probed data for comparison. A: 2 GHz, B: 18 GHz.

(a) CF: Cold FET, $V_g = 0\text{V}$, $V_d = -2\text{V}$
--- Measured in fixture
— Lumped model
- - - Distributed model
... RF-probed data
Radius is "1" for S11, S22, and S12.

(b) HF Hot FET, $V_g = 4\text{V}$, $V_d = -3.7\text{V}$
--- Measured in fixture
— Lumped model
- - - Distributed model
Radius is "1" for S11, S22, and S12; "2" for S21.

(c) Parasitics extraction between RF-probed and fixture-mounted data. The via hole inductance is for a pair on 100 μm substrate. For one via hole, it is approximately 0.03 nH.

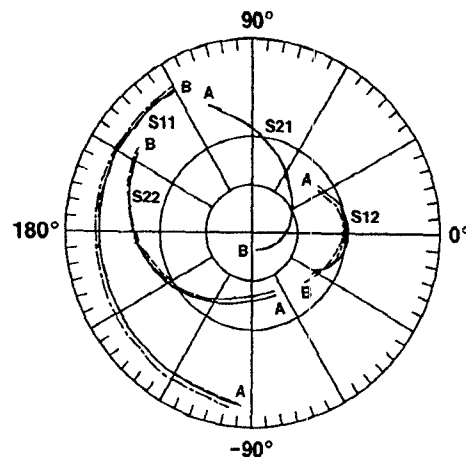


FIG. 5. A sample fitting of a 1600 μm cell (eight fingers) at the same bias point as Figure 4(b). Both lumped and distributed fittings are shown. We have maintained very close to the same distributed parameters. The lumped parameters can also be scaled for the elementary 400 μm cell, except drain, gate inductances and C_{ds} . The pad capacitances and the via hole inductances are also different. A: 2 GHz, B: 18 GHz. Radius is "1" for S11 and S22; "4" for S21; and "0.2" for S12.

— Measured in fixture
— Lumped model
- - - Distributed model

TABLE 2. Lumped and distributed elements of a 1600 μm cell (eight-fingered). The bias point is the same as in Fig. 4(b).

	BIAS DEPENDENT						BIAS INDEPENDENT									
	C_{dq}	C_{qs}	g_m	R_{ds}	R_s	τ	R_0	L_0	C_{sc}	R_d	R_s	R_0	L_0	C_{ds}	C_d	L_v
LUMPED	.115	1.19	.066	101	1.57	6.5	.62	.013	.016	.4	1.1	NA	.021	.36	NA	.026
DISTRIBUTED	.070	.82	.045	178	1.95	6.2	.74	.35	.005	.41	1.51	2.1	.4	.186	.024	.016

BOND PARASITICS						
	$C_{p,ad1}$	$C_{p,ad2}^*$	C_{go}	C_{do}	L_{bg}	L_{bd}
LUMPED	.036	.078	.04	.049	.23	.21
DISTRIBUTED	.030	.031	.04	.049	.23	.21

* L_v is modified by air bridge inductance in lumped element model. Distributed parameters are all per mm, except bond parasitics, τ and L_v . Distributed parameters are all even mode, except bond parasitics and L_v . Even mode value for L_v is that of a single via hole, which is .032 nH in this case.

- + C_{pad2} is modified by drain finger capacitance and drain manifold capacitance in lumped element model.

MANIFOLD + AIR BRIDGE PARASITICS (FIG. 3)							
C ₁	C ₂	C ₃	C ₄	C ₅	L ₁	L ₂	L ₃
.0021	.0038	.0065	.0033	.006	.011	.008	.0012

Gates are approximately 45 μm apart. Air bridge is treated as microstrip lines 40 μm wide and 2.5 μm high with air dielectric.

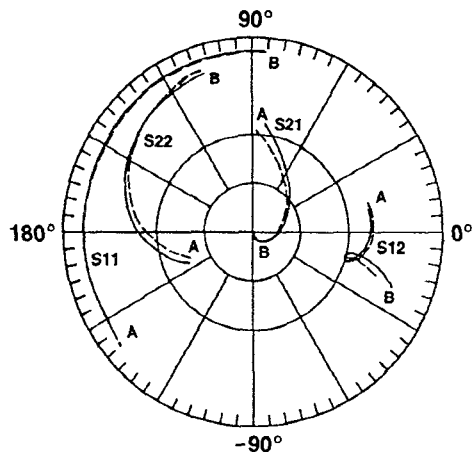


FIG. 6. A sample fitting of a 3200 μm cell (16 fingers) with a distributed model. The scaled up lumped element model could not be fitted with the measured S-parameters as good as the distributed model. Radius is "1" for S11 and S22; "4" for S21; and "0.1" for S12. A: 2 GHz, B: 18 GHz.